

Effect of heavy ion irradiation on the interface traps of AlGaN/GaN high electron mobility transistors

Zheng-Zhao Lin(林正兆), Ling Lü(吕玲), Xue-Feng Zheng(郑雪峰), Yan-Rong Cao(曹艳荣), Pei-Pei Hu(胡培培), Xin Fang(房鑫), and Xiao-Hua Ma(马晓华)

Citation: Chin. Phys. B, 2022, 31 (**3**): 036103. DOI: 10.1088/1674-1056/ac11e4
Journal homepage: http://cpb.iphy.ac.cn; http://iopscience.iop.org/cpb

What follows is a list of articles you may be interested in

Helium-hydrogen synergistic effects on swelling in *in-situ* multiple-ion beams irradiated steels

Haocheng Liu(刘昊成), Jia Huang(黄嘉), Liuxuan Cao(曹留煊), Yue Su(苏悦), Zhiying Gao(高智颖), Pengfei Ma(马鹏飞), Songqin Xia(夏松钦), Wei Ge(葛伟), Qingyuan Liu(刘清元), Shuang Zhao(赵双), Yugang Wang(王宇钢), Jinchi Huang(黄金池), Zhehui Zhou(周哲辉), Pengfei Zheng(郑鹏飞), and Chenxu Wang(王晨旭)

Chin. Phys. B, 2021, 30 (**8**): 086106. DOI: 10.1088/1674-1056/abfcca

Influence of temperature and alloying elements on the threshold displacement energies in concentrated Ni-Fe-Cr alloys

Shijun Zhao(赵仕俊)

Chin. Phys. B, 2021, 30 (**5**): 056111. DOI: 10.1088/1674-1056/abf10d

Bulk and surface damages in complementary bipolar junction transistors produced by high dose irradiation

J Assaf

Chin. Phys. B, 2018, 27 (**1**): 016103. DOI: 10.1088/1674-1056/27/1/016103

Irradiation effects of graphene and thin layer graphite induced by swift heavy ions

Zeng Jian, Liu Jie, Zhang Sheng-Xia, Zhai Peng-Fei, Yao Hui-Jun, Duan Jing-Lai, Guo Hang, Hou Ming-Dong, Sun You-Mei

Chin. Phys. B, 2015, 24 (**8**): 086103. DOI: 10.1088/1674-1056/24/8/086103

Electric field modulation technique for high-voltage AlGaN/GaN Schottky barrier diodes

Tang Cen, Xie Gang, Zhang Li, Guo Qing, Wang Tao, Sheng Kuang

Chin. Phys. B, 2013, 22 (**10**): 106107. DOI: 10.1088/1674-1056/22/10/106107

Effect of heavy ion irradiation on the interface traps of AlGaN/GaN high electron mobility transistors

Zheng-Zhao Lin(林正兆)[1], Ling Lü(吕玲)[1,†], Xue-Feng Zheng(郑雪峰)[1], Yan-Rong Cao(曹艳荣)[2], Pei-Pei Hu(胡培培)[3], Xin Fang(房鑫)[1], and Xiao-Hua Ma(马晓华)[1]

[1] *School of Microelectronics, Xidian University, Xi'an* 710071, *China*
[2] *School of Mechano-Electronic Engineering, Xidian University, Xi'an* 710071, *China*
[3] *Institute of Modern Physics, Chinese Academy of Sciences (CAS), Lanzhou* 730000, *China*

(Received 2 June 2021; revised manuscript received 2 July 2021; accepted manuscript online 7 July 2021)

AlGaN/GaN high electron mobility transistors (HEMTs) were irradiated with heavy ions at various fluences. After irradiation by 2.1 GeV ^{181} Ta^{32+} ions, the electrical characteristics of the devices significantly decreased. The threshold voltage shifted positively by approximately 25% and the saturation currents decreased by approximately 14%. Defects were induced in the band gap and the interface between the gate and barrier acted as tunneling sites, which increased the gate current tunneling probability. According to the pulsed output characteristics, the amount of current collapse significantly increased and more surface state traps were introduced after heavy ion irradiation. The time constants of the induced surface traps were mainly less than 10 μs.

Keywords: gallium nitride, radiation effects, defects, pulse testing

PACS: 61.80.–x, 61.72.uj **DOI:** 10.1088/1674-1056/ac11e4

1. Introduction

Gallium nitride (GaN) based devices are widely used in optoelectronics and power applications. In particular, AlGaN/GaN high electron mobility transistors (HEMTs) are considered as excellent candidates for future power devices because high carrier concentration and electron mobility can be achieved with the two-dimensional electron gas (2DEG) produced by the polarization effect.[1–5] Because the displacement threshold energy of GaN is high, GaN has more effective anti-radiation properties than other semiconductor materials.[6,7] Therefore, AlGaN/GaN HEMTs have obvious advantages in environments with extremely high levels of radiation, in which radiation effects and long-term reliability are important concerns.

Since 2000, numerous studies have been conducted to investigate the effects of radiation on AlGaN/GaN HEMTs.[8,9] The defects introduced by proton, electron, neutron, and heavy ion irradiation at the gate metal/barrier layer interface cause the interface state charge or discharge effect, which shifts the threshold voltage to positive values. Additionally, these irradiation defects increase the probability of electrons crossing the barrier, which increases in the gate-leakage current. Furthermore, irradiation defects in the 2DEG channel layer can capture electrons, thus decreasing the 2DEG density and the saturated drain current.[10–15]

In space, the energy and fluence range of heavy ions are respectively < 10 GeV and 10^5–10^7 particles·cm^{-2}/day.[16] Therefore, practical insights can be gained from studying the effects of heavy ion irradiation on devices. Heavy ions cause single event effects (SEEs), and permanent structural damage in device materials, thereby affecting the stability of the devices.[17–21] Since 2007, researchers have used heavy ions to simulate SEEs. Studies have demonstrated that GaN devices can tolerate high levels of radiation tolerance under total ionizing dose, and enhance low dose rate sensitivity and SEE irradiation.[22,23] Most studies are still focusing on the displacement damage. The degradation phenomenon was found to depend on the ion type, angle, circuit capacitance and manufacturing lot.[24] Microscopic damage can be observed in devices irradiated with heavy ions by using a transmission electron microscope. Sasaki *et al.* observed dislocation rings in devices that were irradiation with 18 MeV Ni ions, but observed no stripe tracks or defects in these devices.[25] Chen *et al.* demonstrated that prior total ionizing dose irradiation with gamma rays exacerbates the SEE of GaN devices induced by subsequent ^{181}Ta^{32+} irradiation.[26] Hu *et al.* were the first to report that ^{209}Bi ions create quasi-continuous tracks in AlGaN/GaN HEMT devices.[27] To elucidate the mechanism of device damage caused by radiation, many studies have been conducted based on two-dimensional technology computer-aided design (2D TCAD).[28]

AlGaN/GaN HEMTs are widely known to be extremely sensitive to surface states, and current collapse is a major factor affecting the RF performance of these devices.[29–31] However, the effect of radiation on the metal/AlGaN layer, specifically the interface traps, has rarely been studied in detail.

Suddenly varying voltages can trap and release surface states, and this forms a "virtual gate" that decreases the drain

†Corresponding author. E-mail: llv@xidian.edu.cn

© 2022 Chinese Physical Society and IOP Publishing Ltd

current, thus affecting device performance.[32,33] Pulsed *I–V* testing is commonly used to measure the amount of current collapse by indirectly characterizing the surface state of the device. In this study, the radiation defects at the metal/AlGaN interface were characterized by pulsed *I–V* testing, and measurements were conducted before and after irradiation to determine the change in trap time constants.

2. Experiments

AlGaN/GaN HEMTs were processed at Xidian University in China. They were grown on sapphire substrates by metal organic chemical vapor deposition. Epitaxial growth was initiated with an AlN nuclear layer, which was followed by a 2 μm undoped GaN buffer and a 22-nm-thick $Al_{0.3}Ga_{0.7}N$ barrier. The ohmic contact comprising Ti/Al/Ni/Au (20/160/55/45 nm) was annealed at 850 °C for 30 s under a nitrogen atmosphere. Schottky contact was realized with Ni/Au/Ni (45/100/20 nm). A 180-nm-thick Si_3N_4 passivation layer was deposited. The gate length and width were 0.2 μm and 50 μm, respectively. A schematic cross section of the AlGaN/GaN HEMTs is shown in Fig. 1.

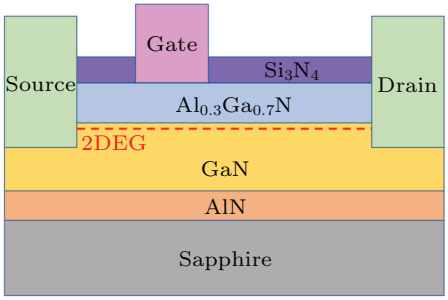


Fig. 1. Schematic cross-section of AlGaN/GaN HEMTs.

The irradiation experiments were performed at the Heavy Ion Research Facility in Lanzhou. To study the effect of heavy ion irradiation on the devices, AlGaN/GaN HEMTs were irradiated with $^{181}Ta^{32+}$ at 2.1 GeV with a total fluence of 1×10^8 ions/cm^2, 1×10^9 ions/cm^2 and 1×10^{10} ions/cm^2 at room temperature. The devices were not biased during the irradiation process.

A Keithley 4200 semiconductor parameter analyzer was used to conduct the DC and pulsed *I–V* measurements at Xidian University. From the test results, we extracted the maximum saturation current, threshold voltage, maximum transconductance, gate-leakage and current collapse to analyze the degradation in electrical properties caused by irradiation. The change in the density of defect states can be determined by comparing the current collapse of the device under different static bias voltages. By comparing the results of tests conducted at different pulse widths, the time constants of the radiation defects can be calculated indirectly.

3. Results and discussion

Figure 2 shows the transfer characteristics of the AlGaN/GaN HEMTs before and after the heavy ion irradiation. The threshold voltage (V_{th}) and maximum transconductance (G_{max}) gradually degraded as the fluence increased. After irradiation by $^{181}Ta^{32+}$ at a fluence of 1×10^{10} ions/cm^2, the electrical characteristics obviously degraded: V_{th} shifted positively by approximately 25% and G_{max} decreased by approximately 8%. Transconductance represents the gate control capability of the device and is an important parameter that affects the frequency characteristics. The degraded G_{max} value can be used to evaluate the extent of damage in the gate area and the decrease in channel electron mobility. Therefore, after heavy ion irradiation, both the gate control capability of the device and the carrier mobility decreased slightly.

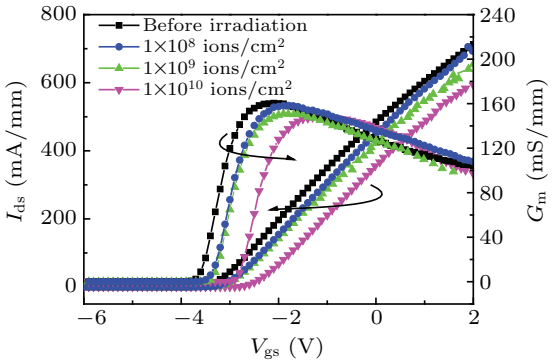


Fig. 2. Transfer characteristics of AlGaN/GaN HEMTs before and after heavy ions irradiation at $V_{ds} = 10$ V. The heavy ions radiation dose varies from 1×10^8 ions/cm^2 to 1×10^{10} ions/cm^2. The left *y*-axis is drain current, and the right *y*-axis is transconductance (G_m).

The output characteristics obtained before and after irradiation are shown in Fig. 3. The maximum saturation current (I_{dsat}) before and after irradiation by heavy ions with a fluence of 1×10^{10} ions/cm^2 at $V_{gs} = 2$ V were 782 mA/mm and 672 mA/mm, respectively. The maximum saturation current was likely degraded by a decrease in electron concentration and saturated carrier velocity.

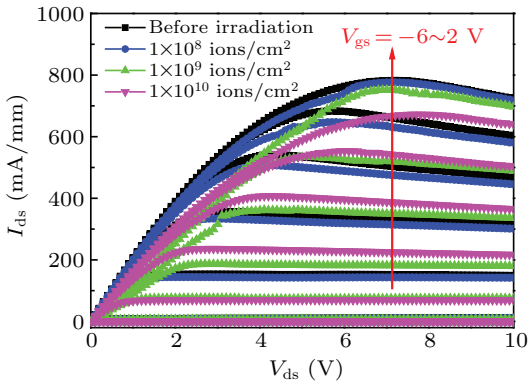


Fig. 3. The output characteristics of AlGaN/GaN HEMTs before and after heavy ions irradiation. The heavy ions radiation dose varies from 1×10^8 ions/cm^2 to 1×10^{10} ions/cm^2. The applied gate bias varies from −6 V to 2 V, and the step is 1 V.

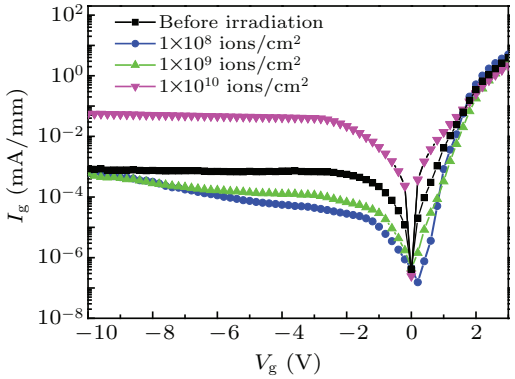


Fig. 4. Gate-leakage of AlGaN/GaN HEMTs before and after the heavy ions irradiation. The heavy ions radiation dose varies from 1×10^8 ions/cm^2 to 1×10^{10} ions/cm^2.

Figure 4 displays the gate-leakage characteristics of the AlGaN/GaN HEMTs before and after irradiation. The results revealed that the gate-leakage currents were slightly improved at the fluences of 1×10^8 ions/cm^2 and 1×10^9 ions/cm^2. This may be attributed to the interaction between $^{181}Ta^{32+}$ and the lattice atoms, which releases a large amount of heat and produces an effect that is similar to thermal annealing, thereby improving the device performance at low fluences. However, other reports stated that it is due to the Kirkendall effect, an increase in the oxygen content at the AlGaN surface after irradiation, which creates a potential barrier for electrons, thus reducing the gate-leakage current.[34,35] At the high fluence of 1×10^{10} ions/cm^2, we observed a significant increase in the gate-leakage current, which maybe caused by the appearance of leakage paths at the interface between the gate metal and barrier layer. The gate forms a Schottky contact, and the Schottky barrier height and ideal factor can be calculated from the forward I_g–V_g characteristics. The barrier height is expressed as follows:

$$\phi_b = \frac{kT}{q}\ln\left(\frac{AA^*T^2}{I_S}\right), \tag{1}$$

where $A^* = 4\pi qk^2m^*/h^3$ is Richardson's constant, A is the area, I_S is the saturation current and T is the temperature. The slope of the plot is related to the ideality factor (n), which is described as follows:

$$n = \frac{\lg e}{(kT/q)\,\text{slope}}. \tag{2}$$

From the results shown in Table 1, the Schottky barrier height remained almost unchanged after irradiation. However, the calculated ideality factor of the device irradiated at a fluence of 1×10^{10} ions/cm^2 was much higher than that before irradiation. The mechanisms of current transport include thermionic emission, generation-recombination, trap-assisted tunneling, and surface leakage. Because the calculated ideality factor is much higher than the expected value, trap-assisted tunneling and surface leakage are the prominent mechanisms. The high-density donor traps introduced unintentionally at the GaN or AlGaN interface reduce the width of the Schottky barrier, which can cause electrons to tunnel easily through the barrier. Irradiation defects induced in the band gap and the interface between the gate and barrier may act as tunneling sites, which increase the gate current tunneling probability.

Table 1. The extracted parameters from forward gate leakage characteristics.

Fluence (ions/cm^2)	Schottky barrier height ϕ_b (eV)	Ideality factor n
Before irradiation	0.39	5.89
1×10^8	0.39	4.07
1×10^9	0.39	5.67
1×10^{10}	0.40	7.61

When heavy ions pass through AlGaN/GaN HEMTs, they transfer energy to the lattice atoms by the ionization and electron-phonon coupling effects, thus inducing radiation defects. According to the simulation results, most of the defects are interstitial atoms, vacancies, Frankel defects, and some defect clusters.[36] Defects cause lattice structure disorder and produce lattice stress. Moreover, defects and defect clusters accumulate along the latent track. According to our previous study, the degradation properties of devices are closely related to the defects introduced by irradiation.[27] As the amount of induced defects increases, the scattering in the carrier transport channel also increases and the effective carrier concentration decreases, which degrades the electrical performance of the device. However, latent tracks can only be found in the devices irradiated with relatively high fluences. Once the latent track is observed, the devices are damaged.

Our experiments revealed that while performance degraded slightly at low fluences, the device still continued to work. As the radiation fluence gradually increased, damage to the device became more serious. At this point, we focused on the effects at the radiation interface.

Figure 5 shows a schematic of the pulsed I–V test method. The three different quiescent bias conditions are $(0,0) = [V_{GSQ} = 0\text{ V}, V_{DSQ} = 0\text{ V}]$, $(-8,0) = [V_{GSQ} = -8\text{ V}, V_{DSQ} = 0\text{ V}]$, and $(-8,10) = [V_{GSQ} = -8\text{ V}, V_{DSQ} = 10\text{ V}]$. If the pulse width is very small relative to the pulse period, the self-heating and trapping effects mainly depend on the choice of the static operating point. When the pulse width is small and the trap release or capture time constant is much smaller than the pulse width, the self-heating and trapping effects of the device can be considered constant and do not change with the pulse voltage. The amount of electrons that are trapped or released increase as the pulse width increases, thus gradually increasing the degree of current collapse. Therefore, it is important to choose an appropriate static operating point and pulse width to analyze the defect trapping effect of the irradiated device.

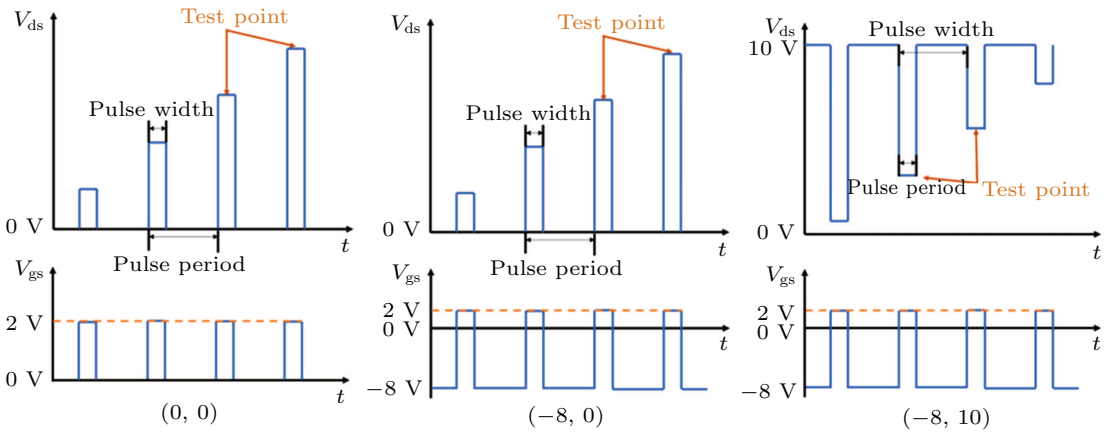


Fig. 5. Schematic of pulsed *I*–*V* testing.

Figure 6 shows the results of pulsed I_D–V_D testing with a pulse width of 500 ns at $V_g = 2$ V before and after irradiation. At (−8,0) and (−8,10) states, the electrons in the channel were depleted and the device was in the off state. Current collapse at (−8,0) and (−8,10) states is likely due to the electrons trapped under the gate and the gate–drain access region, respectively. Because current collapse did not occur in the (0,0) state, the (0,0) state was taken as the reference state for current collapse. The greater the surface state density, the more electrons that are trapped and the greater the current collapse caused by the surface state. Therefore, the surface state density of the gate and gate–drain region can be indirectly measured by the pulsed test method. To quantitatively study the current collapse, the amount of current collapse is defined according to Eq. (3). The drain current is selected in the deep saturation region ($V_{DS} = 10$ V).[37]

$$\text{Collapse} = \frac{I_D(0,0) - I_D(V_{GSQ}, V_{DSQ})}{I_D(0,0)} \times 100\%. \tag{3}$$

As shown in Fig. 6, the drain currents at (−8,0) and (−8,10) states were lower than that at the (0,0) state, because electrons were injected from the gate to the gate–drain region and were trapped by the surface states, causing current collapse. At the (−8,10) state, the electric field is larger on the drain side of the gate edge, more electrons are injected into the gate–drain region, and more electrons are trapped by the surface state, so the pulse output current is the smallest. The amount of current collapse after irradiation was greater than that before irradiation, especially at the fluence of 1×10^{10} ions/cm^2. This is likely due to the introduction of more surface state traps by irradiation. The higher the surface state density, the higher the quantity of electrons that are trapped and the more serious the current collapse. Augaudy *et al.* posited that these effects are mainly related to the time constants associated with the electron capture and emission process.[38]

Figure 7 shows the output characteristics of the devices under DC conditions and at different quiescent bias conditions. The pulse width varied from 500 ns to 100 μs, and the pulse period was 1 ms. Before irradiation, the drain current under pulsed testing was higher than that under DC testing. As the pulse width increased, the drain current decreased. The decrease in $I_{d-pulse}$ is generally considered due to the captured electrons in the traps, and electron capture by traps may occur when the voltage changes to the test voltage. When the pulse width is 500 ns, there is insufficient time for the surface traps to capture electrons; therefore, the pulse current $I_{d-pulse}$ is much larger than the DC current I_{d-dc}. As the pulse width increases, the surface traps have sufficient time to capture electrons; therefore, the pulse current decreases.

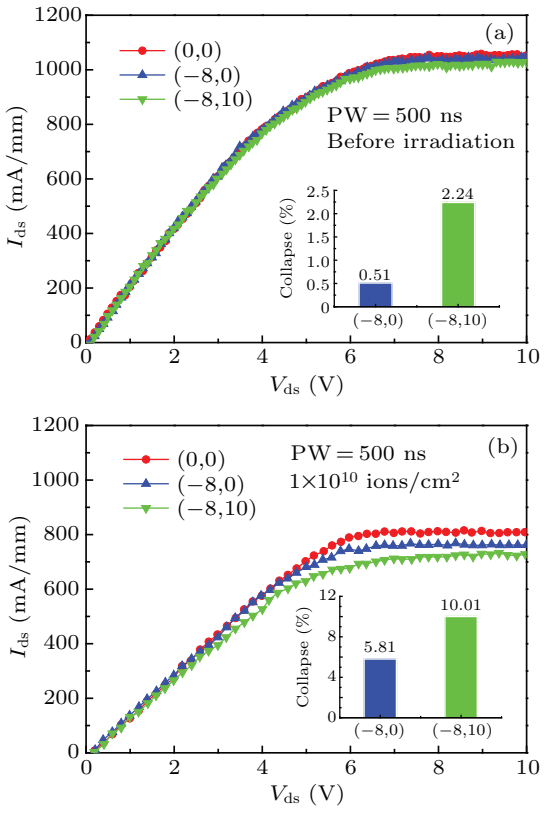


Fig. 6. Comparison of different quiescent bias condition with the same pulse width (pulse width (PW) = 500 ns), (a) before irradiation (b) 1×10^{10} ions/cm^2.The current collapse amounts are shown in the insets.

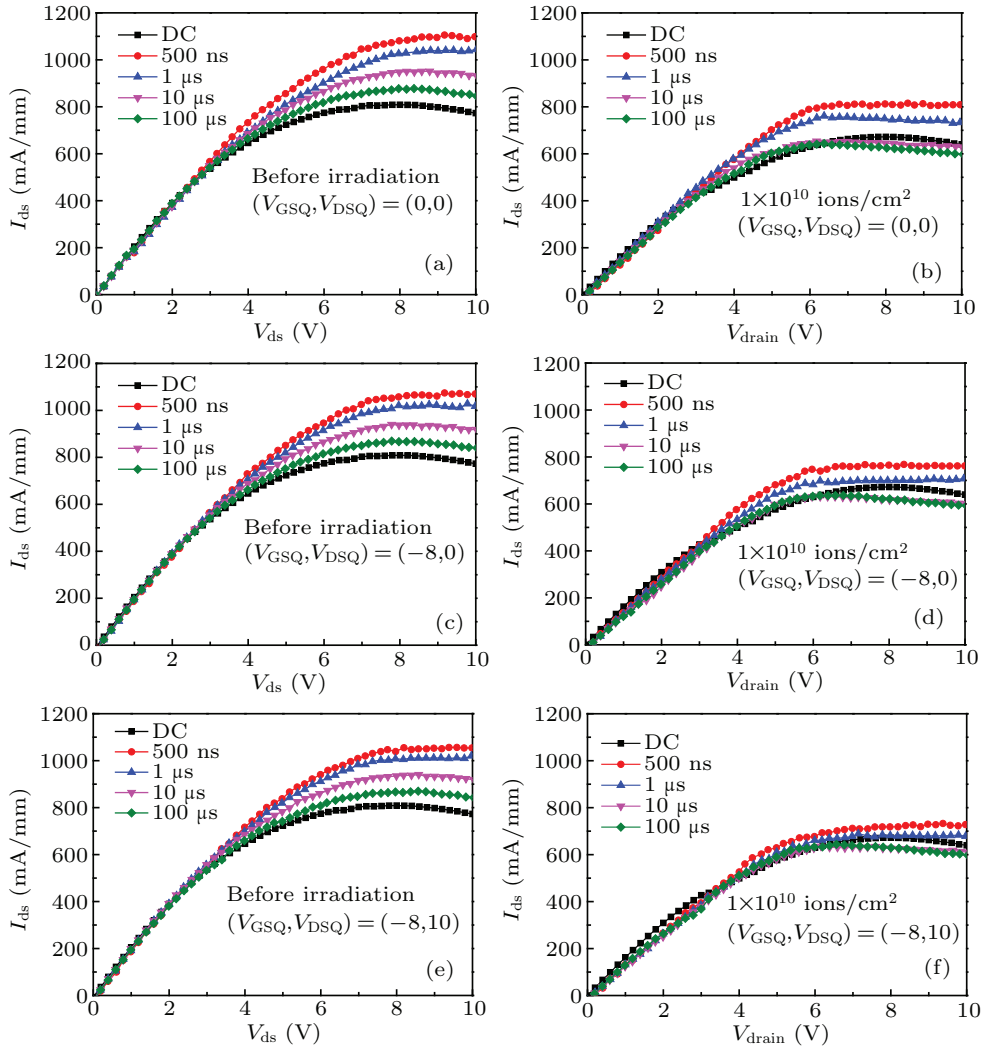


Fig. 7. The output characteristics ($V_{gs} = 2$ V) in different pulsed conditions before and after irradiation, (a) and (b) are for (0,0) state, (c) and (d) are for (−8,0) state, (e) and (f) are for (−8,10) state.

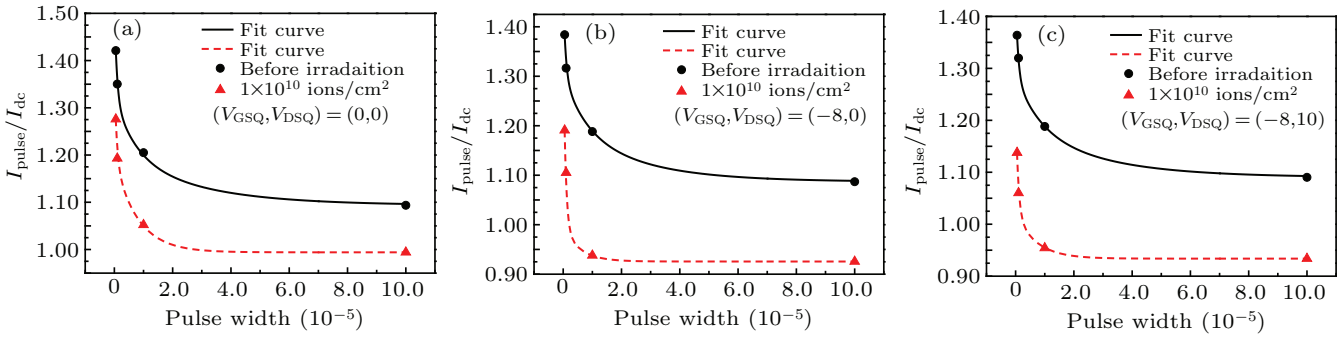


Fig. 8. The relationship between $I_{d-pulse}/I_{d-dc}$ and pulse width at different quiescent bias conditions, (a) (0,0) state, (b) (−8,0) state, (c) (−8,10) state.

As shown in Fig. 7, the difference in pulse current between the pulse widths of 10 μs and 100 μs was the smallest after heavy ion irradiation at the fluence of 1×10^{10} ions/cm^2. After heavy ion irradiation, there were few surface states with time constants in the range of 10 μs $< \tau <$ 100 μs and many surface traps with time constants in the range of 500 ns $< \tau <$ 10 μs.

We used Eqs. (4)–(6) to fit the variation in $I_{d-pulse}/I_{d-dc}$ with pulse width to obtain the corresponding trap time constant. In these equations, I_{DC} is the DC drain current, while τ_1, τ_2 and τ_3 are the trap time constants. Moreover, I_1, I_2 and I_3 are the fitting constants,[29]

$$I_D(t) = I_{DC}\left[1 - I_1\exp(-t/\tau)\right], \tag{4}$$

$$I_D(t) = I_{DC}\left[1 - I_1\exp(-t/\tau_1) - I_2\exp(-t/\tau_2)\right], \tag{5}$$

$$I_D(t) = I_{DC}[1 - I_1\exp(-t/\tau_1) - I_2\exp(-t/\tau_2) - I_3\exp(-t/\tau_3)]. \tag{6}$$

Figure 8 shows the relationship between $I_{d-pulse}/I_{d-dc}$

and the pulse width at different quiescent bias conditions. The aforementioned equations were used to fit the experimental data. The fitted trap time constants are shown in Fig. 9. Equation (6) was used to fit the experimental data obtained before irradiation, while Eq. (4) was used for the data obtained after irradiation. The results revealed that traps with time constants in the range of 10 μs $< t <$ 100 μs disappeared after the irradiation.

In summary, more surface state traps are introduced after heavy ion irradiation. Moreover, the time constants of the surface traps induced by heavy ion irradiation are concentrated between 500 ns and 10 μs.

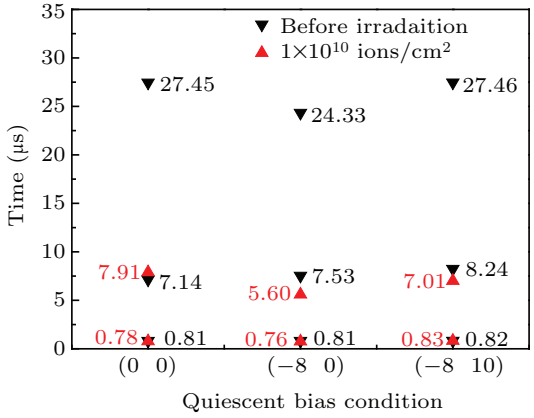


Fig. 9. The fitting trap time constant of devices before and after irradiation.

4. Conclusion

In this paper, the evolution of interface traps at the gate/AlGaN layer in AlGaN/GaN HEMTs under 2.1 GeV $^{181}Ta^{32+}$ heavy ion irradiation was investigated in detail. The characteristics of the interface traps were determined by pulsed *I*–*V* testing. A quantitative comparison of current collapse revealed that irradiation introduced more surface traps. However, by comparing the different pulse widths at the same quiescent operating point, we found that heavy ion irradiation reduced the amount of surface trap states with time constants between 10 μs and 100 μs. Therefore, heavy ion irradiation introduced more trap states with time constants less than 10 μs. The results presented herein facilitate our understanding of the effects of heavy ion irradiation on interface traps in AlGaN/GaN HEMTs.

Acknowledgements

Project supported by the National Natural Science Foundation of China (Grant Nos. 12035019 and 11690042) and Science Challenge Projects (Grant No. TZ2018004).

References

[1] Amano H, Baines Y, Beam E, *et al.* 2018 *J. Phys. D: Appl. Phys.* **51** 163001
[2] Flack T J, Pushpakaran B N and Bayne S B 2016 *J. Electron Mater.* **45** 2673
[3] Asif Khan M, Bhattarai A, Kuznia J N and Olson D T 1993 *Appl. Phys. Lett.* **63** 1214
[4] Ambacher O, Foutz B, Smart J, Shealy J R, Weimann N G, Chu K, Murphy M, Sierakowski A J, Schaff W J, Eastman L F, Dimitrov R, Mitchell A and Stutzmann M 2000 *J. Appl. Phys.* **87** 334
[5] Baliga B J 2013 *Semicond. Sci. Technol.* **28** 074011
[6] Ionascut-Nedelcescu A, Carlone C, Houdayer A, von Bardeleben H J, Cantin J L and Raymond S 2002 *IEEE Trans. Nucl. Sci.* **49** 2733
[7] Nord J, Nordlund K and Keinonen J 2003 *Phys. Rev. B* **68** 184104
[8] Pearton S J, Hwang Y S and Ren F 2015 *JOM* **67** 1601
[9] Polyakov A Y, Perton S J, Frenzer P, Ren F, Liu L and Kim J 2013 *J. Mater. Chem. C* **1** 877
[10] Luo B, Johnson J W, Ren F, Allume K K, Abernathy C R, Pearton S J, Wowchack A M, Polley C J, Chow P P, Schoenfeld D and Baca A G 2002 *Appl. Phys. Lett.* **80** 604
[11] Hwang Y-S, Liu L, Ren F, Polyakov A Y, Smirnov N B, Govorkov A V, Kozhukhova E A, Kolin N G, Boiko V M, Vereyovkin S S, Ermakov V S, Lo C F, Laboutin O, Cao Y, Johnson J W, Kargin N I, Ryzhuk R V and Pearton S J 2013 *J. Vac. Sci. Technol. B* **31** 022206
[12] Katz E J, Lin C H, Qiu J, Zhang Z, Mishra U K, Cao L and Brillson L J 2014 *J. Appl. Phys.* **115** 123705
[13] Jiang R, Zhang E X, McCurdy M, Chen J, Shen X, Wang P, Fleetwood D M, Schrimpf R D, Kaun S W, Kyle E C H, Speck J S and Pantelides S T 2017 *IEEE Trans. Nucl. Sci.* **64** 218
[14] Pearton S J, Ren F, Patrick E, Law M E and Polyakov A Y 2015 *ECS J. Solid State Sci. Technol.* **5** Q35
[15] Chen J, Puzyrev Y S, Jiang R, Zhang E X, McCurdy M W, Fleetwood D M, Schrimpf R D, Pantelides S T, Arehart A R, Ringel S A, Saunier P and Lee C 2015 *IEEE Trans. Nucl. Sci.* **62** 2423
[16] Lei Z, Guo H, Tang M, Zeng C, Chen H and Zhang Z 2016 *IEEE Proceedings of 16th European Conference on Radiation and Its Effects on Components and Systems (RADECS)*, September 19–23, 2016, Bremen, Germany
[17] Zerarka M, Austin P, Toulon G, Morancho F, Arbess H and Tasselli J 2012 *IEEE Trans. Electron Dev.* **59** 3482
[18] Abbate C, Busatto G, Iannuzzo F, Mattiazzo S S, Sanseverino A, Silvestrin L, Tedesco D and Velardi F 2015 *Microelectron. Reliab.* **55** 1496
[19] Kuboyama S, Maru A, Shindou H, Ikeda N, Hirao T, Abo H and Tamura T 2011 *IEEE Trans. Nucl. Sci.* **58** 2734
[20] Stoffels S, Melotte M, Haussy M, Venegas R, Marcon D, Van Hove M and Decoutere S 2013 *IEEE Trans. Nucl. Sci.* **60** 2712
[21] Samsel I K, Zhang E X, Hooten N C, Funkhouser E D, Bennet W G, Reed R A, Schrimpf R D, McCurdy M W, Fleetwood D M, Weller R A, Vizkelethy G, Sun X, Ma T P, Saadat O I and Palacios T 2013 *IEEE Trans. Nucl. Sci.* **60** 4439
[22] Bazzoli S, Girard S, Ferlet-Cavrois V, Baggio J, Paillet P and Duhamel O 2009 *IEEE Proceedings of RADECS European Conference on Radiation & Its Effects on Components & Systems,* September 14–18, 2009, Brugge, Belgium, p. 623
[23] Lidow A, Nakata A, Rearwin M, Strydom J and Zafrani A M 2014 *Radiation Effects Data Workshop IEEE*, July 14–18, 2014, Paris, France
[24] Scheick L 2014 *IEEE Trans. Nucl. Sci.* **61** 2881
[25] Sasaki H, Hisaka T, Kadoiwa K, Oku T, Onoda S, Ohshima T, Taguchi E and Yasuda H 2018 *Microelectron. Reliab.* **81** 312
[26] Chen S Y, Yu X, Lu W, Yao S and Guo Q 2020 *Chin. Phys. Lett.* **37** 046101
[27] Hu P P, Liu J, Zhang S X, Maaz K, Zeng J, Zhai P F, Xu L J, Cao Y R, Duan L J, Li Z Z, Sun Y M and Ma X H 2018 *Nucl. Instrum. Methods. Phys. Res. Sect. B* **430** 59
[28] Zerarka M, Austin P, Bensoussan A, Morancho F and Durier A 2017 *IEEE Trans. Nucl. Sci.* **64** 2242
[29] Vetury R, Zhang N Q Q, Keller S and Mishra U K 2001 *IEEE Trans. Electron Dev.* **48** 560
[30] Binari S C, Klein P B and Kazior T E 2002 *Proc. IEEE* **90** 1048
[31] Joh J and Alamo J A del 2011 *IEEE Trans. Electron Dev.* **58** 132
[32] Meneghesso G, Rampazzo F, Kordos P, Verzellesi G and Zanoni E 2006 *IEEE Trans. Electron Dev.* **53** 2932
[33] Zhang A P, Rowland L B, Kaminsky E B, Tilak V, Grande J C, Teetsov J, Vertiatchikh A and Eastman L F 2003 *J. Electron. Mater.* **32** 388
[34] Smigelskas A D and Kirkendall E O 1947 *Trans. AIME* **171** 130
[35] Koehler A D, Specht P and Anderson T J 2014 *IEEE Trans. Electron Dev.* **35** 1194
[36] Ziegler J F, Ziegler M D and Biersack J P 2010 *Nucl. Instrum. Methods Phys. Res. Sect. B* **268** 1818
[37] Ghosh S, Das S, Dinara S M, Bag A, Chakraborty A, Mukhopadhyay P, Jana S K and Biswas D 2018 *IEEE Trans. Electron Dev.* **65** 1333
[38] Augaudy S, Teyssier R P, Di Forte-Poisson M A, Cassette S, Dessertenne B and Delage S L 2001 *IEEE MTT-S International Microwave Symposium Digest* **1** 427